



Research paper

Direct synthesis of mesoporous SRL-POM@MOF-199@MCM-41 and its highly catalytic performance for the oxidesulfurization of DBT

Si-Wen Li^a, Zhi Yang^a, Rui-Min Gao^b, Gai Zhang^c, Jian-she Zhao^{a,*}^a Key Laboratory of Synthetic and Natural Functional Molecule Chemistry of Ministry of Education, Shaanxi Key Laboratory of Physico-Inorganic Chemistry, College of Chemistry & Material Science, Northwest University, Xi'an, Shaanxi 710127, China^b Research Institute of Shaanxi Yanchang Petroleum Group Corp. Ltd., Xi'an 710075, China^c School of Materials and Chemical Engineering, Xi'an Technological University, Xi'an 710021, China

ARTICLE INFO

Keywords:

Surfactant-type heteropolyacid
Metal-organic framework
MCM-41 molecular sieve
Oxidative desulfurization
Reusability

ABSTRACT

With the increasing aim of deep desulfurization of fuel, a kind of novel surfactant-type heteropolyacid $[(\text{CH}_3)_2(\text{C}_n\text{H}_{2n+1})\text{N}(\text{CH}_2)]_2[\text{POM}]$ (SRL-POM, $n = 10, 12, 14$ and 16) was successfully synthesized and then it template self-construction of MOF-199 in the pore of MCM-41 (SRL-PMM). This catalyst was exploited to act as a stable heteropolyacid-based one, under the dual protection functions of MOF-199 and MCM-41. Structure was characterized by X-ray diffraction (XRD), Fourier transform infrared (FT-IR), X-ray photoelectron spectroscopy (XPS), N_2 adsorption-desorption, scanning electron microscopy (SEM), transmission electron microscopy (TEM) and so on. Direct oxidation of dibenzothiophene (DBT) using O_2 was performed by this surfactant-type heteropolyacid catalyst with 100% selectivity in the oxidation of DBT to sulfones under the optimal conditions and shown a better reusability. Furthermore, the kinetic studies reveal that the oxidative desulfurization can present a pseudo first-order kinetic process, and this work offers an alternative for oxidative desulfurization of real oil samples as well.

1. Introduction

With the increasingly stringent regulations and fuel specifications of petroleum refining industry in worldwide, the environmental friendly fuels which own the low sulfur content (< 10 ppm) have motivated an increase in research [1,2]. However, the conventional hydrodesulfurization (HDS) only shows high activity to remove thiols, sulfides and disulfides, which also need high temperatures, high pressures and high hydrogen consumption [3]. The alternative deep desulfurization processes have been widely investigated, including biodesulfurization [4,5], selective adsorption desulfurization [6,7], extraction desulfurization [8] and oxidative desulfurization [9–11]. Among them, the oxidative desulfurization is the most promising method owing to its advantages like mild and simple operation conditions as well as the high efficient in removing heterocyclic sulfur-containing compounds such as dibenzothiophene (DBT) and its derivatives, especially 4,6-dimethylbenzothiophene (4,6-DMDBT). By means of this procedure, in the presence of an oxidant and appropriate catalyst, the refractory sulfur compounds are converted in sulfoxide and/or sulfone with subsequent removal of these products by polar extraction for achieving ultra-low-sulfur fuel [12]. Although conventional solvents,

which are usually volatile organic compounds, can be used as extractants, their further environmental and safety concerns greatly limit their applicants. Ionic liquids (ILs) have proved to be successful as sustainable extraction solvents due to their good extraction performance for thiophenic S-compounds, clear phase separation and negligible solubility in fuel oils [13–15].

Heteropolyacids (POMs) belong to a large class of metal-oxygen cluster anions which presents various structures, including the Keggin type that represents the most employed in catalysis, for the stability of POMs combined with their structural flexibility to incorporate various elements in their framework making them attractive catalysts [16,17]. Amphiphilic quaternary ammonium micelles of POMs, with a surfactant surface and a POM core, have gradually become worldwide attention, especially for the applicant in ODS processes [19]. This structure could possibly take advantage of its large lipophilic hydrocarbon part, which can help in hydrophobic distribution of the catalyst in oil, in favor of less mass transfer resistance and faster reaction rate. Jiang and co-workers have reported the oxidation of DBT with O_2 as the oxidant using reverse micellar system, where an amphiphilic catalyst $[\text{C}_{18}\text{H}_{37}\text{N}(\text{CH}_3)_3]_7[\text{PW}_{10}\text{Ti}_2\text{O}_{38}(\text{O}_2)_2]$ acts as both the surfactant and the catalyst [20]. It could catalytically decrease sulfur level in diesel from 500 ppm

* Corresponding author.

E-mail address: jszhao@nwu.edu.cn (J.-s. Zhao).

to 1.0 ppm at ambient pressure and moderate temperature. However, reduced attention has been paid to the low surface area ($1\text{--}10 \text{ m}^2/\text{g}$) of these surfactant containing ODS system. Therefore, dispersing them on solid supports with high surface areas is most important. A number of attempts have been made, with the goal of creating a discrete and uniform catalytic site on the inner walls of the porous system via host-guest interactions. Zaki Eldin Ali Abdalla and co-workers have introduced the $(\text{C}_{19}\text{H}_{42}\text{N})_4\text{H}_3(\text{PW}_{11}\text{O}_{39})$ into mesoporous silica by direct synthesis, and the catalyst showed high oxidation activity for oxidative desulfurization of DBT, which reduced its sulfur contents from 500 ppm to 0.2 ppm in 90 min [21]. Their research group have also prepared $(\text{Bu}_4\text{N})_4\text{H}_3(\text{PW}_{11}\text{O}_{39})/\text{MCM-41}$ by impregnation methods under reflux conditions, in which $(\text{Bu}_4\text{N})_4\text{H}_3(\text{PW}_{11}\text{O}_{39})$ was grafted onto silica surface face through W-Si-O linkage [22]. The material was found to be highly active and reusable catalyst for almost 100% DBT removal rate. MOFs have been shown to be effective supports to incorporate POMs to form efficient heterogeneous catalysts [23,24]. Susana Ribeiro and co-workers have encapsulated the tetrabutylammonium salt of phosphotungstic acid, $\text{TBA}_3\text{PW}_{12}\text{O}_{40}$, in the metal-organic framework MIL-101 [25]. The sulfur removal from model oil with a sulfur content of 500 ppm reached 100% within 1 h for DBT and the catalyst could be recycled three times with only a slight decrease in the catalytic performance.

In this work, a kind of surfactant-type heteropolyacid catalyst, SRL-POM@MOF-199@MCM-41 (SRL-PMM), was designed, aiming to achieve the advantages of both the porous materials support and surfactant Keggin-type POMs associated quaternary ammonium salt. Using the right pore sizes, the difunctional porous materials, MOF-199 and MCM-41, were used to fix the active species (POMs) by the template self-construction of MOF-199 in the pores of MCM-41 and POM is in the center. This design is aiming to obtain the more stability structure, leading to improvements for deep oxidative desulfurization.

2. Experimental

2.1. Materials and instrumentation

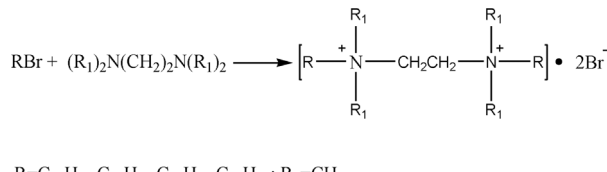
All solvents and reagents which are used in synthesized procedure were analytical purity and were used as received. The raw materials of catalysts were purchased as follows: disodium hydrogrnn phosphate (Xi'an Chemical Works), sodium tungstate, tetramethylammonium hydroxide, bromodecane, bromododecane, bromotetradecane and bromohexadecane (Aldrich), sodium molybdate (Adamas), 1, 3, 5-benzenetricarboxylic (Acros Organics), cupric nitrate, cetyltrimethyl ammonium bromide and concentrated H_2SO_4 (Tianjing Chemical Works), N,N,N',N' -tetramethyl ethylenediamine (Sinopharm Chemical Reagent Co., Ltd). The chemicals for desulfurization experiments, DBT (J & K technology), octane (Tianjing Fuchen chemical reagent factory) and $[\text{Bmim}] \text{BF}_4^-$ (J & K technology), were used as received.

Elemental analyses for C, H, N, were executed on PE2400 and ^1H NMR spectra were measured with a Bruker ARX400 spectrometer at ambient temperature in using TMS as internal reference. Fourier transform infrared spectra (FT-IR) were measured as KBr pellets on the EQUINOX-55 FTIR spectrometer from German Bruker Company. Power X-ray diffraction patterns were collected on a Rigaku, D/max-2550/PC (Rigaku, Japan) using Cu K α radiation from a 2 θ range of 2–40° varied at 0.02°/step. The support MCM-41 and the composite were degassed overnight at 100 °C prior to analysis. The Brunauer-Emmett-Teller (BET) method was utilized to calculate the special surface area, which was obtained on TriStar II 3020 degassed at 423 K for 6 h. The morphology of the catalysts was observed via Scanning Electron Microscopy (SEM, TM3000) and samples were coated with gold to make them conductive. Transmission electron microscopic (TEM) images were generated with Philips TecnaiG2 F20 instrument at an accelerating voltage of 200 kV. X-ray photoelectron spectroscopy (XPS) was used to analyze the catalysts using K-Alpha on PHI-1600 from US

Thermo Electron Corporation. Inductively coupled plasma atomic emission spectroscopy (ICP-AES) was performed on a Thermo Scientific IRIS Advantage ICP emission spectrometer.

2.2. Preparation of the catalyst

2.2.1. Preparation of SRL



SRLs, a kind of surfactant, were synthesized as follows: The bromodecane (26.14 ml, 0.15 mmol) was dropwised to the N,N,N',N' -tetramethyl ethylenediamine (7.44 ml, 0.05 mmol) in a three-neck flask and then added 30 ml absolute ethanol as solvent. Under the room temperature, the mixture was refluxed and stirred for 48 h. The light yellow raw product was obtained followed evaporation and dried in vacuum at 50 °C overnight. After recrystallization in the mixture of absolute ethanol/ethy 1 acetate, the white power was filtered, washed and then dried at 50 °C in vacuum (yielding 74%).

Anal. Calcd for $\text{C}_{26}\text{H}_{58}\text{N}_2\text{Br}_2$ (557.80, SRL-1): C, 55.90; H, 10.38; N, 5.017. Found: C, 55.93; H, 10.40; N, 5.020. ^1H NMR (CDCl_3): $\delta = 0.87$ (t, 6H, $\text{CH}_2\text{CH}_2\text{CH}_3$), $\delta = 3.51$ (s, 12H, NCH_3), $\delta = 3.75$ (t, 4H, $\text{NCH}_2\text{CH}_2\text{N}$), $\delta = 1.80$ (m, 4H, $\text{CH}_2\text{CH}_2\text{CH}_2\text{N}$), $\delta = 1.27$ (m, 24H, $(\text{CH}_2)_4$), $\delta = 1.38$ (m, 4H, $\text{CH}_3\text{CH}_2\text{CH}_2$), $\delta = 3.34$ (t, 4H, $\text{CH}_2\text{CH}_2\text{CH}_2\text{N}$).

Anal. Calcd for $\text{C}_{30}\text{H}_{66}\text{N}_2\text{Br}_2$ (614.67, SRL-2): C, 58.62; H, 10.82; N, 4.560. Found: C, 58.34; H, 10.91; N, 4.328. ^1H NMR (CDCl_3): $\delta = 0.90$ (t, 6H, $\text{CH}_2\text{CH}_2\text{CH}_3$), $\delta = 3.49$ (s, 12H, NCH_3), $\delta = 3.83$ (t, 4H, $\text{NCH}_2\text{CH}_2\text{N}$), $\delta = 1.84$ (m, 4H, $\text{CH}_2\text{CH}_2\text{CH}_2\text{N}$), $\delta = 1.27$ (m, 32H, $(\text{CH}_2)_8$), $\delta = 1.35$ (m, 4H, $\text{CH}_3\text{CH}_2\text{CH}_2$), $\delta = 3.33$ (t, 4H, $\text{CH}_2\text{CH}_2\text{CH}_2\text{N}$).

Anal. Calcd for $\text{C}_{34}\text{H}_{74}\text{N}_2\text{Br}_2$ (670.77, SRL-3): C, 60.88; H, 11.12; N, 4.180. Found: C, 60.39; H, 11.22; N, 4.217. ^1H NMR (CDCl_3): $\delta = 0.87$ (t, 6H, $\text{CH}_2\text{CH}_2\text{CH}_3$), $\delta = 3.50$ (s, 12H, NCH_3), $\delta = 3.80$ (t, 4H, $\text{NCH}_2\text{CH}_2\text{N}$), $\delta = 1.86$ (m, 4H, $\text{CH}_2\text{CH}_2\text{CH}_2\text{N}$), $\delta = 1.20$ (m, 40H, $(\text{CH}_2)_4$), $\delta = 1.38$ (m, 4H, $\text{CH}_3\text{CH}_2\text{CH}_2$), $\delta = 3.35$ (t, 4H, $\text{CH}_2\text{CH}_2\text{CH}_2\text{N}$).

Anal. Calcd for $\text{C}_{38}\text{H}_{82}\text{N}_2\text{Br}_2$ (726.88, SRL-4): C, 62.79; H, 11.37; N, 3.85. Found: C, 62.64; H, 11.58; N, 3.554. ^1H NMR (CDCl_3): $\delta = 0.88$ (t, 6H, $\text{CH}_2\text{CH}_2\text{CH}_3$), $\delta = 3.49$ (s, 12H, NCH_3), $\delta = 3.65$ (t, 4H, $\text{NCH}_2\text{CH}_2\text{N}$), $\delta = 1.78$ (m, 4H, $\text{CH}_2\text{CH}_2\text{CH}_2\text{N}$), $\delta = 1.26$ (m, 48H, $(\text{CH}_2)_4$), $\delta = 1.37$ (m, 4H, $\text{CH}_3\text{CH}_2\text{CH}_2$), $\delta = 3.30$ (t, 4H, $\text{CH}_2\text{CH}_2\text{CH}_2\text{N}$).

2.2.2. Preparation of SRL-POM

Pure Keggin-type POM of $\text{H}_3\text{PMo}_6\text{W}_6\text{O}_{40}$ was prepared following the method in our previous work [26].

SRL-POM was prepared following the procedure described as below. A solution of SRL (0.9 mmol dissolved in 10 ml deionized water) was added dropwise to the aqueous solution of previously prepared POM (0.6 mmol in 10 ml deionized water), stirring under 80 °C for 6 h. After cooling to the room temperature, the yellow solid was isolated by filtration and dried at 50 °C in vacuum (yielding 95%).

2.2.3. Preparation of SRL-POM@MCM-41 (SRL-PMC)

The pure MCM-41 was synthesized also followed the reported method [27]. SRL-PMC, which was obtained by adding 0.6 g MCM-41 into the anhydrous ethanol solution with 0.4 g of SRL-POM dissolved in a little acetonitrile, was constant stirred for 16 h. Following the dip for

24 h and filtration, the yellow solid products were dried under 110 °C overnight and calcined under 300 °C for 2 h.

2.2.4. Preparation of SRL-PMM

0.1815 g (0.75 mmol) of Cu(NO₃)₂·3H₂O and 0.1 g SRL-POM were added into 5 ml distilled water containing 0.1 g MCM-41. Then, 0.2718 g (1.5 mmol) (CH₃)₄NOH·5H₂O (TMA) and 0.0946 g (0.75 mmol) 1, 3, 5-benzenetricarboxylic (BTC) were added to stir for addition 30 min. Transferring the mixture into an autoclave equipped with 10 ml of PTEF lined and heated to 180 °C for 16 h, the light green powders could be obtained.

2.3. Oxidative desulfurization processes

The ODS experiments were carried out in a closed 200 ml three-neck flask connected with a pump to share oxygen, a magnetic stirrer and a reflux condenser. The blowing oxygen was used as oxidant, while the model oils were obtained by dissolving DBT in octane, with their initial S-content all being 2000 ppm. 100 ml of model oil, 10 ml [Bmim]BF₄ and 0.15 g catalysts were stirred vigorously at a constant speed. Reaction products were collected every 30 min after the centrifugation, which were collected the upper clear phrase. Then the removal of sulfur compounds was soon calculated after the analysis of gas chromatography Agilent GC 6890 and followed the equation below (C₀ and C stand for the initial and final concentration of S-compounds, respectively), the DBT conversion rate (η) was obtained.

$$\eta = [(C_0 - C)/C_0] \times 100\%$$

$$\text{TOF}(\text{h}^{-1}) = \text{moles of sulfur (per hour)}/\text{moles of catalyst (SRL - POM)} \times 100\%$$

3. Results and discussion

3.1. Catalyst characterization

The XRD patterns of SRL-POM and SRL-PMM are shown in Fig. 1, taking SRL-3 as an example. There are several peaks which emerge mainly at 17, 23, 28, 29.3, 32.5 and 36, showing that the surfactant-type heteropolyacid was retained after immobilization. As for the low angle, a series of obvious peak at 2θ = 2.1°, due to (100) index, while the other two weak peaks below 8° suggest a hexagonal symmetry of MCM-41. The modification with SRL-POM is still mesoporous and similar to the pure MCM-41. The strongest peaks appear at 2θ = 6 and 12, reflecting a typical feature of MOF-199. The existence of

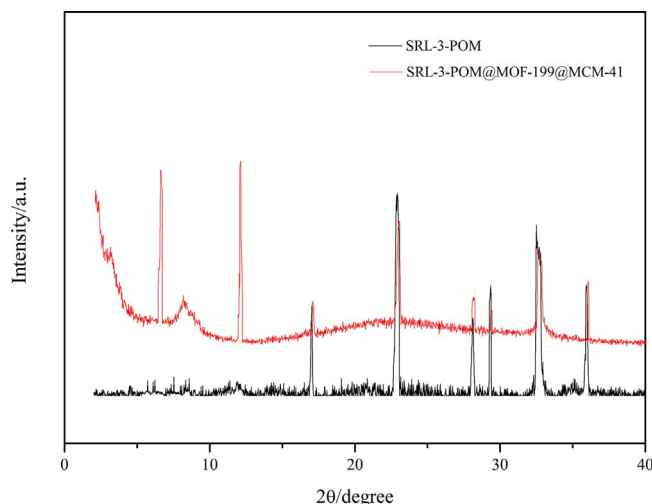


Fig. 1. The X-Ray powder patterns of samples.

characteristic peaks belonging to the three parts, SRL-POM, MOF-199 and MCM-41, is a good evidence of the formation on the as-designed structure.

Fig. 2a depicts FT-IR spectrum of different heteropolyacid with surfactants. The spectrum of SRL-POM at 2871 and 2965 cm⁻¹ are assigned to the symmetric and asymmetric stretching vibrations of –CH₂ group, while the peaks at 1482 cm⁻¹ are attributed to C–H scissoring vibrations of CH₃–N⁺ moiety, indicating the presence of amino-functionalized groups in SRL-POM. This peaks show a slight shift among the different chain groups in SRL may be due to the surfactant interactions between POM and SRL which effect on CH₃–N⁺ vibration. The structure of Keggin type heteropolyacid consist of a PO₄ tetrahedron that surrounded by four (Mo/W)₃O₁₀ groups formed by the edge sharing atoms, being the characteristics fingerprint FT-IR bands between 750 and 1100 cm⁻¹. The spectrum of SRL-POM shows bands at 1098 cm⁻¹, which is attributed to the asymmetric vibrations of P–O of tetrahedral PO₄, while the bands at 965, 873 and 802 cm⁻¹ are attributed to the stretching modes of the terminal Mo/W–O_b edge sharing Mo/W–O_b–Mo/W and corner sharing Mo/W–O_c–Mo/W units, respectively. In Fig. 2b spectra of SRL-POM loaded porous materials are shown, taking SRL-3-POM as an example. The Si–O–Si bending vibration and asymmetric stretching vibrations of MCM-41 are appeared at 460 and 1080 cm⁻¹. The band at 962 cm⁻¹ is ascribed to the stretching vibration of Si–OH. Thus, the overlapped cases by frequencies of MCM-41 to the SRL-POM are obvious. The two bands at ~1440 and ~1590 cm⁻¹ correspond with the ν(COO) symmetric and asymmetric stretching of the carboxylate, while another band centered at 728 cm⁻¹ results in the groups on benzene ring after replacing by copper atoms, which belong to the characteristic band on the MOF-199. Nevertheless, in comparison with each others in Fig. 2b, the presence of the typical bands of the SRL-POM as well as MOF-199 should be strongly evidenced as a result of that they are persevered even after anchoring to MCM-41, obtaining the as-designed catalysts SRL-PMM.

For the further investigation of structural integrity of SRL-POM unit and its interaction with porous materials supports, MOF-199 and MCM-41, ³¹P CP-MAS NMR of samples has been studied. As shown in Fig. 3, synthesized SRL-PMM shows resonance signal at –10.7 ppm, which is close to the value (–11.1 ppm) of the pure SRL-POM. Based on the above results, they are in agreement with the conclusion that the structure of the Keggin remained intact after formation of the SRL-PMM.

The diffuse reflectance UV-vis spectra of the catalysts are shown in Fig. 4. All the samples show two absorption bands, one around 230 nm and the other one around 310 nm. The first one was observed, mainly attributed to the O–P transition, and the second broad band may be assigned to the charge transfer transition of the bridging oxygen to the metal, indicating the presence of octahedral coordination in extra-framework [28]. As for the as-designed sample, SRL-PMM, the obvious broad bands around 750 nm is mainly attributed to the ligand field transition (d-d) in the presence of MOF-199. The findings above also imply the structure of the samples we designed.

The surface morphologies of MCM-41 and SRL-PMM were examined by SEM analysis (Fig. 5a and b), while TEM analysis was used to further determine structural information on the as-prepared sample (Fig. 5c). The surface of the fresh MCM-41 is smooth and appears spherical shape particles. And the whole morphology of SRL-PMM remains the same except for relatively small and intensive, which attributes to the increase of loading results. It can be seen from the Fig. 4c that the TEM image shows the high ordered hexagonal mesostructure in accordance with the pure MCM-41, even at high SRL-POM loadings. What is more, the clearly dark colored fine particles are uniformly distributed inside the pores of MCM-41, which is also consistent with the above results that the SRL-POM units have been successfully introduced into the pores of inner wall of material which constructs the uniform active center.

The composition and its chemical status of the SRL-PMM sample are investigated by X-ray photoelectron spectroscopy (XPS) analysis. The

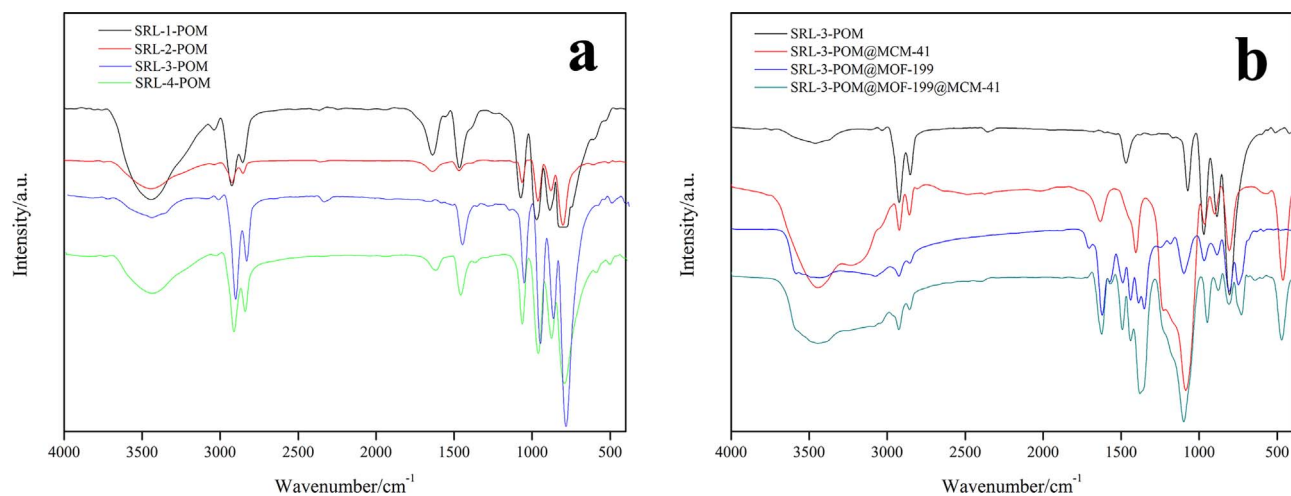


Fig. 2. FT-IR spectra of heteropolyacids (a) before (SRL-POM) (b) after immobilization.

results (Fig. 6) show the peaks corresponding to P_{2p} (BE = 130 and 131 eV), Mo_{3d} (BE = 231 and 234 eV), W_{4f} (BE = 34.5 and 36.5 eV) in Keggin heteropolyacid anion and a N peak at 401.5 eV due to the quaternary ammonium cation. The Si_{2p} and O_{1s} peaks indicate the existence of MCM-41, while Cu_{2p} peaks identified at 933 and 954 eV are attributed to the Cu²⁺ in the MOF-199.

The nitrogen adsorption-desorption isotherms of the MCM-41, SRL-PMC and SRL-PMM samples are shown in Fig. 7. It is clear that all the samples exhibit type IV isotherms with H1 hysteresis loop which are attributed to qualities of mesoporous materials. This implied that the ordered mesostructure remained after supporting active species into the MCM-41. However, the volumes adsorbed inflected sharply at a relative pressure (P/P₀) at 0.95 for pure MCM-41 and extended to a lower relative pressure (P/P₀) at ca. 0.92. The physical property parameters (Table 1) demonstrate that the as-designed sample, SRL-PMM, has a specific surface area of 281 m²/g lower than that of the unmodified

MCM-41 (732 m²/g), and the most probable pore volume decreased to 0.12 cm³/g, proving that the SRL-PMO are formed on the internal surface of the mesoporous channels. Compared with the SRL-PMC, the relative more adsorption volume also confirmed the successful incorporation of the MOF-199 after the self-assembly, even wrapping the modified heteropolyacid in the big size pores of MCM-41. Very notably in view of the Table 1, the N element content in the SRL-PMM is 1.95% by ICP-AES experiments, which is consistent with the above result that SRL-POM has been successfully introduced into the pores.

TGA profiles of pure SRL-POM and SRL-PMM catalysts are presented in Fig. 8. The as-synthesized SRL-POM comprises three main weight loss steps up to 800 °C. As the results shown, there was 14.8% mass loss before 319 °C, which corresponded to the combined water in heteropolyacid. The catalyst decomposed about 10.9% mass loss in the second step from 315 °C to 477 °C, indicating that the loss of a long chain of quaternary ammonium salt in surfactant-type heteropolyacid. Then,

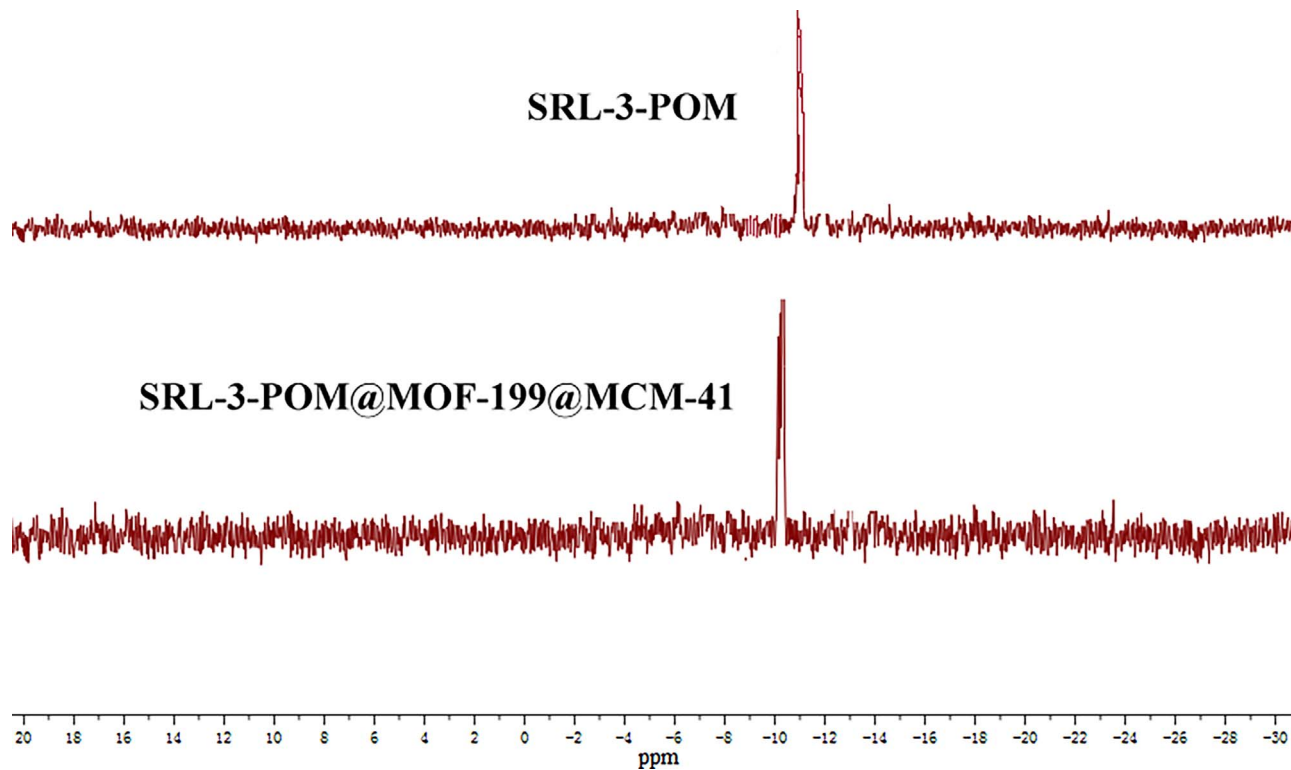


Fig. 3. ³¹P NMR spectrum of SRL-POM and SRL-PMM.

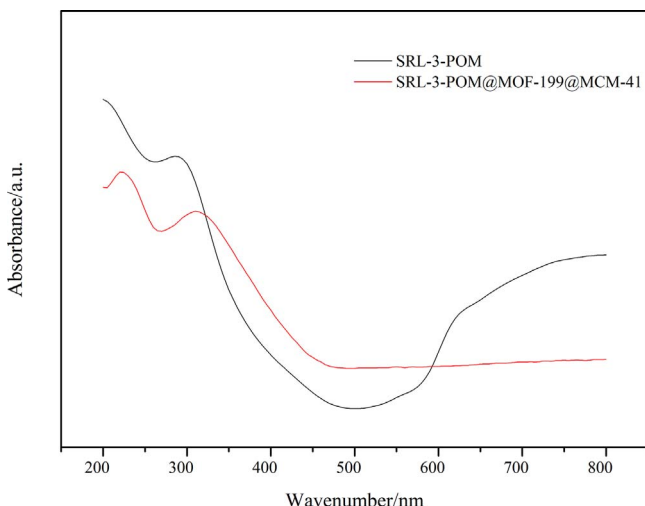


Fig. 4. UV-vis spectra of SRL-POM and SRL-PMM.

after 477 °C, the heteropolyacid decomposed and final reminder was metal oxide. The weight loss of SRL-PMM catalyst in the same temperature range is evidently lower than that of pure SRL-POM, as would be expected from the presence of the SRL-PMO in the composite.

3.2. Influence of different catalyst on removal of DBT

Table 2 depicts the removal efficiency of DBT over different catalyst systems. It can be seen, the catalyst without anyone of MOF-199, MCM-41 or SRL-POM, exhibited poor desulfurization efficiency. In all studies, O₂ was used as oxidant and reactions were performed under 60 °C, 500 rpm agitation rate, and with an amount of catalyst 1.5 g/L. Notably, the removal efficiency of pure SRL-POM can reach 37.6%, without the porous materials supporting, it could be great loss following the experiments to reduce the DBT removal rate. While after loading them on the supporters, MCM-41 or MOF-199, the significant improvement indicated that the introduction of supporters played an important role in the desulfurization efficiency of catalysts. But for the wantonly agglomerated state of heteropolyacid species in the relatively large pores of MCM-41, following leading the self-assembled of metal-organic framework MOF-199, the dually supported catalyst SRL-PMM shows the high quality efficiency on DBT removal and repeat utilization. Among the series of SRL-PMM, the SRL-3-PMM shows the 100% DBT removal rate after 150 min. As we all know, the long carbon chain of the quaternary ammonium cations from the hybrid catalysts could facilitate the desulfurization, while the overlong may have the adverse results for the steric effects [29]. Thus, SRL-3-PMM was selected as the representative catalyst to further optimize other reaction conditions in the following experiments.

To make further comparison, the catalytic performance of several representative heteropolyacids catalysts under similar reaction

conditions (DBT as single sulfur compound in model oil) was listed in Table 3. Remarkably, the surfactant-type POM modified porous materials system with the dual-protected function effect showed outstanding in removal of sulfur compound from model fuel under mild conditions.

3.3. Influence of the preparation condition on SRL-POM loading amount

The effect of SRL-POM loading amount on the oxidative desulfurization of the model fuel oil is shown in Fig. 9. It is clear that the DBT removal rate increased firstly and then declined. For the total amount of the SRL-PMM catalyst is 0.15 g, the SRL-POM mass fraction (wt%) varies among various catalysts. When the SRL-POM content is higher than 40%, a much higher conversion of DBT is obtained (100%). These phenomena attributed to the different content of active species. However, when the SRL-POM was more than 40%, the obvious decrease was shown for the very unfavorable for the catalytic activity. The excessive blockage of pores may show the opposite direction we expected, so the 40% SRL-POM in SRL-PMM catalyst was used in the subsequent study of ODS process.

3.4. Influence of the reaction conditions on removal of DBT

The effect of catalyst dosage on oxidative desulfurization of the model oil is shown in Fig. 10a. It was found that the catalyst dosage does have a marked influence on the process efficiency, which indicating that it is difficult to achieve deep sulfur level without catalyst. Increasing the catalyst dosage enhances the conversion of DBT. However, the curve saturates after reaching to 1.5 g/L. Further increase in the dosage of the active catalyst shows a slight effect on DBT removal.

The different agitation rates were proceeded on the removal of DBT, exhibiting the feature of the phase-transfer agents. The obvious change of the sulfur removal from 300 rpm to 500 rpm was achieved, increasing from 89.1% to nearly 100%. As the higher agitation rate beyond, the sulfur removal hardly altered and declined gradually. This may be ascribed to the break of the mass transfer resistance before the 500 rpm, as the SRL was believed to play a major role in the formation and stabilization of emulsion during the oxidative process, while the more quick agitation rate causes the volatilization rate of solvent leading the decreased of the DBT removal rate. Thus, the optimal agitation rate kept at 500 rpm during the experiments.

The influence of the oxidant flow rate on the DBT conversion over SRL-PMM is presented in Fig. 10c. Under the same condition, the efficiency of the oxidative desulfurization is superior, especially at 750 ml/min within 150 min. The DBT conversion rate increases with the O₂ flow rate (from 250 to 750 ml/min), while at the relative high rate, the desulfurization efficiency shows a decreased trend. The reason may be that the shortened contact time of O₂ with DBT and the increased volatilization rate of solvent. Hence, considering the economic factors and the desulfurization efficiency, the 750 ml/min was chosen as the optimum.

To study the desulfurization efficiencies at different sulfur levels,

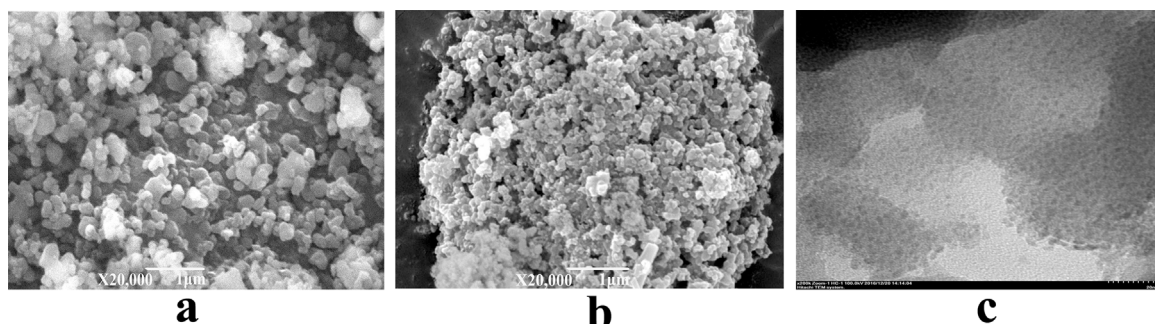


Fig. 5. SEM images of (a) MCM-41, (b) SRL-PMM and TEM image of (c) SRL-PMM.

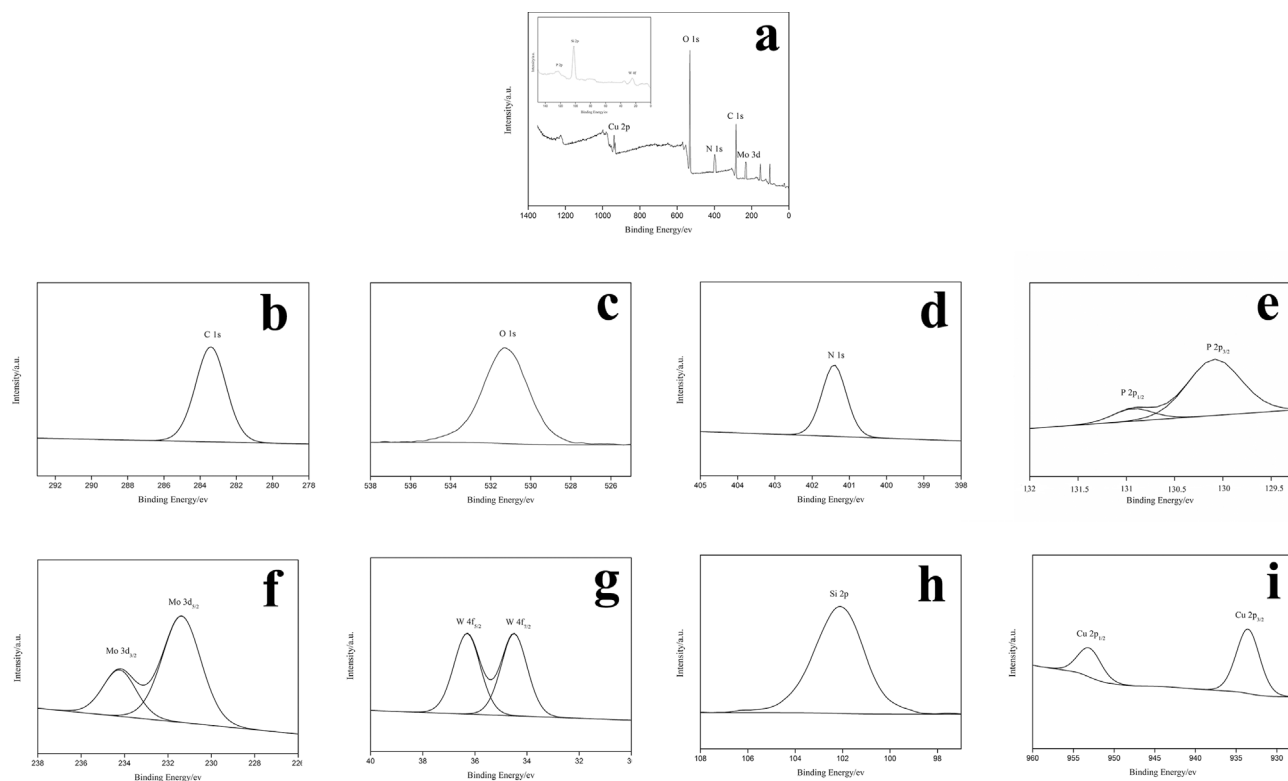


Fig. 6. XPS spectra of the SRLPMM sample. (a) Survey of the sample; (b) C 1s; (c) O 1s; (d) N 1s; (e) P 2p; (f) Mo 3d; (g) W 4f; (h) Si 2p and (i) Cu 2p.

the experiments were performed using different concentrations (800, 1200, 1600, 2000, 2400 and 2800 ppm), while other variables were kept constant, as shown in Fig. 10d. The rate of removal increases when the DBT concentration increases, indicating that the removal of DBT depends on its initial concentration. It can be seen that from the 800 ppm to 2000 ppm, the same final desulfurization efficiency of 100% was achieved, the difference of which was the time. Especially, the completely DBT removal rate under 800 ppm was obtained in 90 min. As the initial sulfur contents increased to 2400 and 2800 ppm respectively, the final desulfurization efficiencies were found to be 93.3% and 90% accordingly. This phenomenon may be due to the decrease of catalytic active sites. The increase in initial sulfur content can speed up the oxidation of DBT and meanwhile deepens the consumption of both species. The desulfurization efficiency will rise when the initial sulfur content is not high, while after a certain high content, the large amount of excessive DBT may not be removed completely leading to the

Table 1
Physical properties parameters of MCM-41, SRL-PMC and SRL-PMM.

Samples	S_{BET} (m^2/g)	V_p (cm^3/g)	D(nm)	N (wt.%) ^a
MCM-41	732	0.66	3.54	
SRL-PMC	457	0.31	3.57	0.17
SRL-PMM	281	0.12	3.62	0.12

^a As determined by ICP-AES experiments.

definitely declined results. So, agreeable effect of DBT removal has been achieved within the initial sulfur content below 2000 ppm.

Influence of reaction temperature on the ODS of the model oil was investigated under the selected conditions above and oxygen as oxidant, as shown in Fig. 11a. It could be found that the desulfurization efficiencies increase with the increment in reaction temperature and

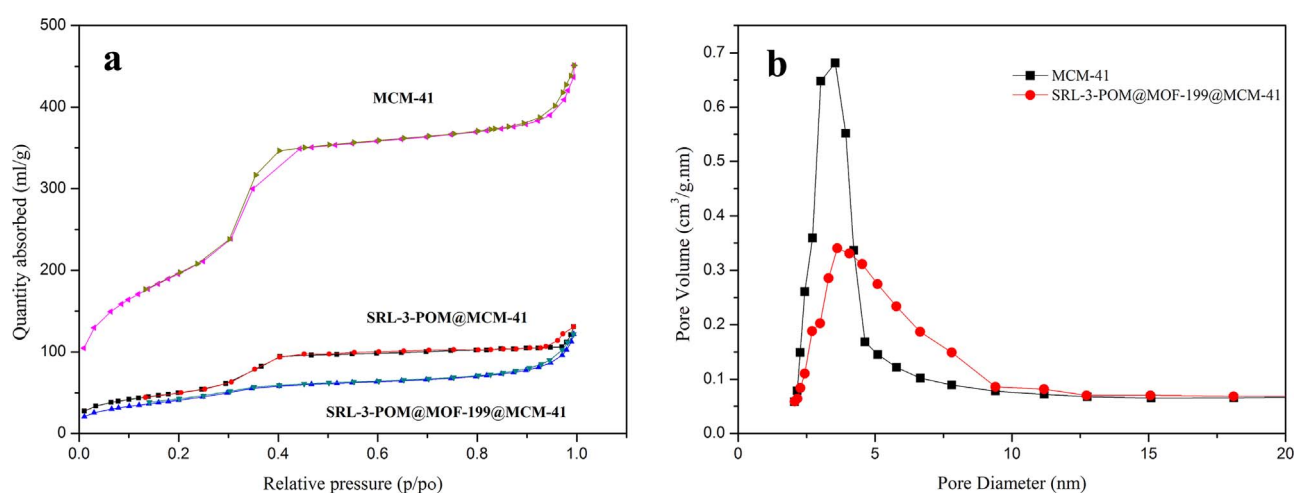


Fig. 7. (a) N_2 adsorption-desorption isotherms of different samples, (b) BJH pore size distribution curves of samples.

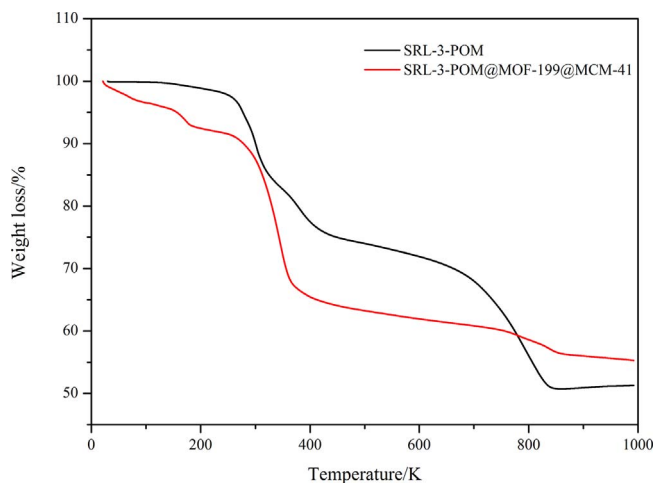


Fig. 8. TGA analysis of SRL-POM and SRL-PMM.

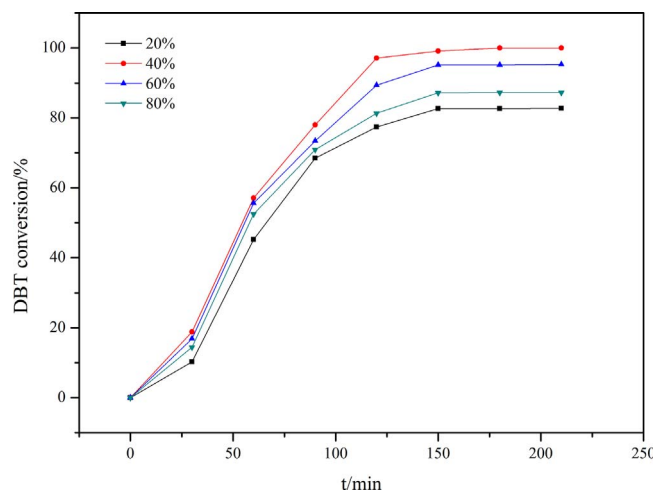
Fig. 9. The conversion of DBT on SRL-PMM under different loading amounts. Conditions: reaction temperature, 60 °C; catalyst dosage, 1.5 g/L; agitation rate, 500 rpm; reaction time, 210 min; O₂ flow rate, 750 ml/min; initial concentration, 2000 ppm.

Table 2

DBT removal of different desulfurization systems.

Entry	Different desulfurization systems	TOF (h ⁻¹)	DBT Conversion rate (%)
1	SRL-POM ^a	15.3	37.6
2	MOF-199@MCM-41	9.4	20.2
3	SRL-POM@MCM-41 ^a	18.7	45.1
4	SRL-POM@MOF-199 ^a	29.1	64.9
5	SRL-1-POM@MOF-199@MCM-41	40.6	87.3
6	SRL-2-POM@MOF-199@MCM-41	48.4	92.8
7	SRL-3-POM@MOF-199@MCM-41	56.1	100
8	SRL-4-POM@MOF-199@MCM-41	45.8	90.5

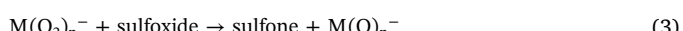
^a Reaction conditions: 1.0 g/L, 150 min, 60 °C, 500 rpm.

temperature does have a significant effect on DBT degradation. The sulfur removal was only 82% at 30 °C, while as the temperature rising, the 60 °C had the highest sulfur removal of DBT reaching to 100%. Lower sulfur removal was obtained at low temperature and the higher sulfur removal was opposite, which mainly ascribed to the increased constant of reaction rate and then the effective collision probability between the catalysts and oxidant leading to the higher DBT removal efficiency. Therefore, in this system, the enhanced temperature benefited for the desulfurization process and the 60 °C was chosen as the economic and efficient condition.

The results were consistent with the catalytic kinetics and the oxidation reaction of DBT followed pseudo-first-order kinetics, as shown in Fig. 11b. The equation is $\ln \frac{C}{C_0} = -kt$, where C_0 and C is the concentration of sulfur at initial and t (min), and k is the rate constant. A linear relationship is obtained when $\ln \frac{C}{C_0}$ versus reaction time is plotted for 60 °C. The apparent activation energy was also derived from the Arrhenius Equation $E_a = RT^2 \frac{d\ln k}{dT}$ and 23.7 kJ/mol was obtained.

3.5. The possible mechanism

A possible mechanism for the catalytic oxidation of DBT by SRL-PMM is shown in Fig. 12. The reaction occurs by simultaneous extraction/oxidation of dibenzothiophene in biphasic system, which ionic liquid emulsion was immiscible with model oil. The DBT in the model oil was first extracted from oil phase into IL phase and oxidized to their corresponding sulfones by the active species, SRL-PMM, simultaneously. The oxidation might proceed including two consecutives stages: the first stage includes $M(O_n^-)$ ($M = Mo$ or W) in SRL-POM obtains oxygen molecular yielding the active peroxy group of heteropolyacid $M(O_2)_n^-$, then one DBT molecule combines with it to gained sulfoxide; secondly, one sulfoxide oxidized to sulfone by $M(O_2)_n^-$. And the catalytic cycle could be achieved following the oxygen molecular regenerated, which could be. The sulfones accumulated in IL phase. After reaction, the desulfurization system quickly divided into two layers and the sulfur-free oil is obtained.



3.6. Recycling of the catalyst

There is no doubt that the recycling of the catalysts is extremely important factors in terms of industrial application. The reaction was cooled to room temperature after 150 min before the catalyst was filtered off. It was known that the [Bmim]BF₄, which functioned as extraction agent, was immiscible with the model oil and the surfactant-type heteropolyacid catalysts was more likely to precipitate in the lower phase during the extraction process. Thus, the ionic liquid with catalysts could be collected easily and removed the residual oil under rotary

Table 3

Comparison of various catalysts for oxidative desulfurization of DBT of model oil.

Entry	Catalyst System	Extractants	Reaction time (min)	Desulfurization efficiency (%)	References
1	HPWA-SBA-15	t-BuOOH	120	97.43	[30]
2	(C ₁₆ min) ₂ Mo ₂ O ₁₁		60	98.4	[31]
3	HPMo/SiO ₂	DMF	150	99.2	[32]
4	CTA-POM/SiO ₂	methanol	90	99.54	[21]
5	C ₁₈ PW ₁₀ Ti ₂ (O ₂) ₂		360	99.8	[20]
6	SRL-PMM	[Bmim]BF ₄	150	100	This work

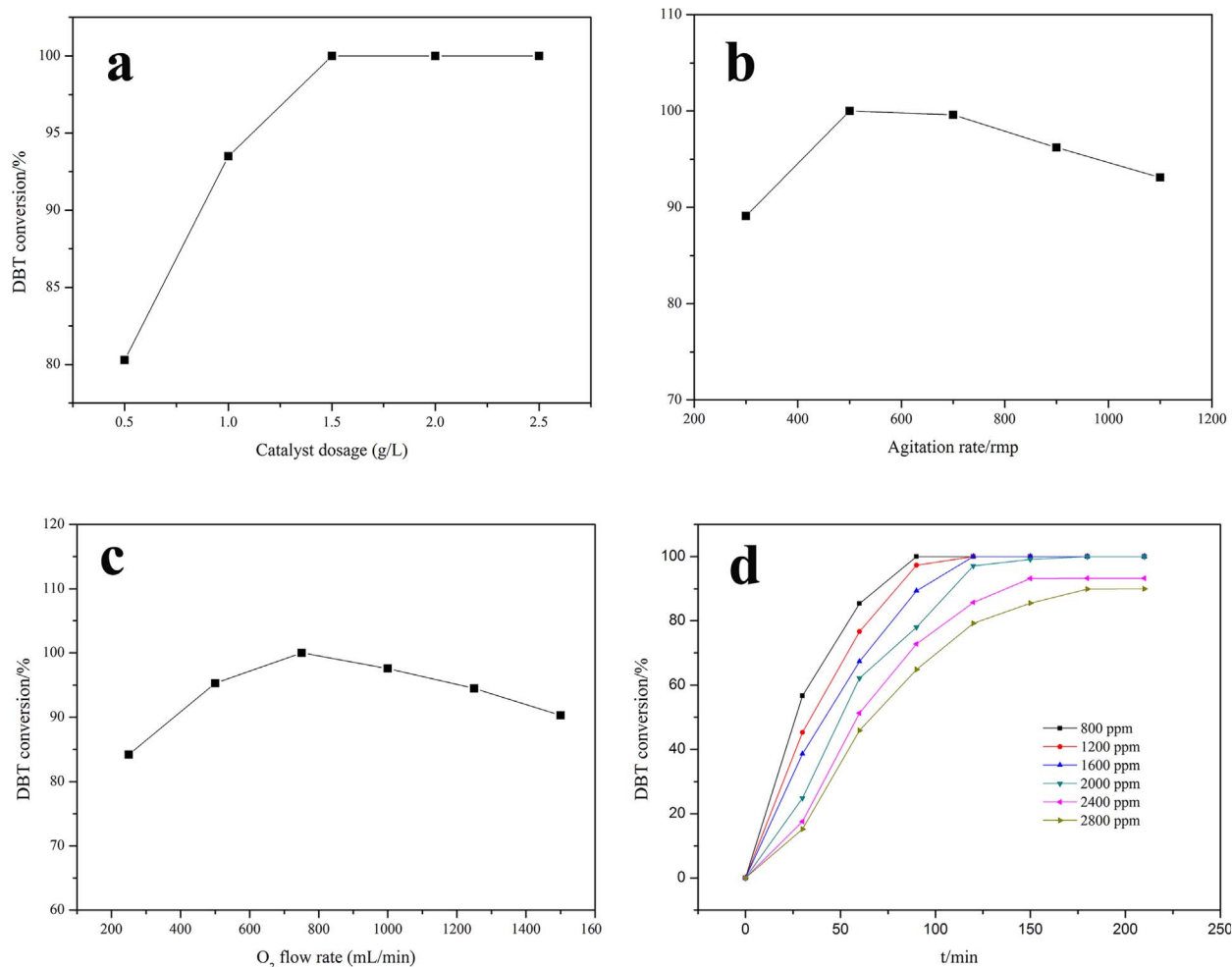


Fig. 10. The research of optimal reaction conditions on SRL-PMM for the deep oxidative desulfurization. Conditions: (10a) loading amount, 40%; reaction temperature, 60 °C; agitation rate, 500 rmp; reaction time, 150 min; O₂ flow rate, 750 mL/min; initial concentration, 2000 ppm; (10b) loading amount, 40%; reaction temperature, 60 °C; catalyst dosage, 1.5 g/L; reaction time, 150 min; O₂ flow rate, 750 mL/min; initial concentration, 2000 ppm; (10c) loading amount, 40%; reaction temperature, 60 °C; agitation rate, 500 rmp; catalyst dosage, 1.5 g/L; reaction time, 150 min; initial concentration, 2000 ppm; (10d) loading amount, 40%; reaction temperature, 60 °C; agitation rate, 500 rmp; catalyst dosage, 1.5 g/L; reaction time, 150 min; O₂ flow rate, 750 mL/min.

evaporation for the following recycle. Thus, except the fresh ionic liquid ([Bmim]BF₄:10 ml) was added at the beginning of desulfurization process, it was not used in each recycle experiment. In other words, we could collect nearly 10 ml ionic liquid after each recycle time with almost no loss, and only the same volumes of fresh model oil is required

to add into the original reaction flask for the next run, which being great benefit for the practical industrial application. It should be pointed out that the agitation rate of 500 rmp must be used so as to avoid the high DBT conversion of mass transfer effect. The results are shown in Fig. 13. It could be seen that the conversion of DBT decreased

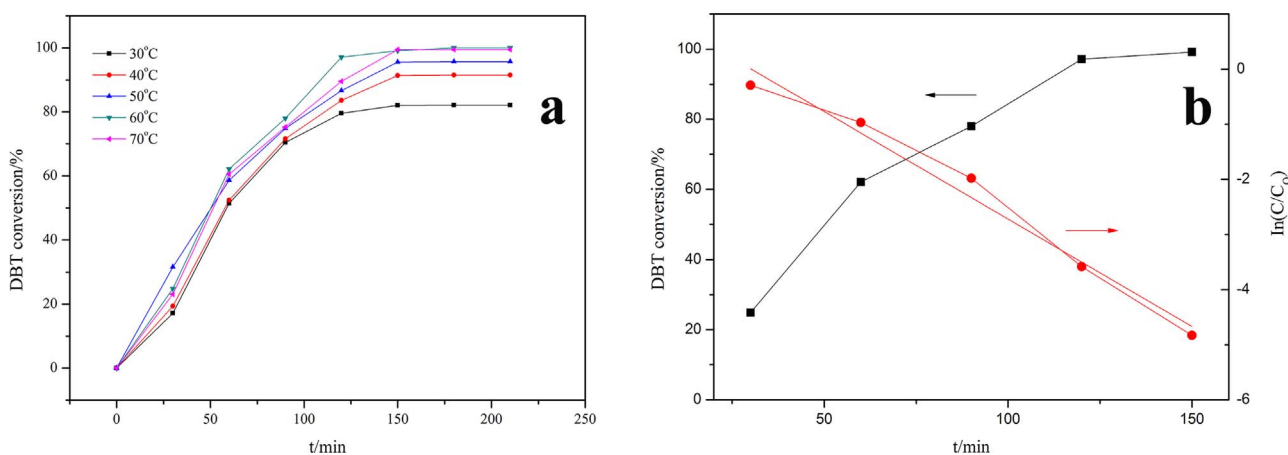


Fig. 11. (a) Effect of temperature on DBT removal; (b) fitting experimental data to the pseudo-first-order rate model. Conditions: loading amount, 40%; reaction temperature, 60 °C; catalyst dosage, 1.5 g/L; agitation rate, 500 rmp; reaction time, 150 min; O₂ flow rate, 750 mL/min; initial concentration, 2000 ppm.

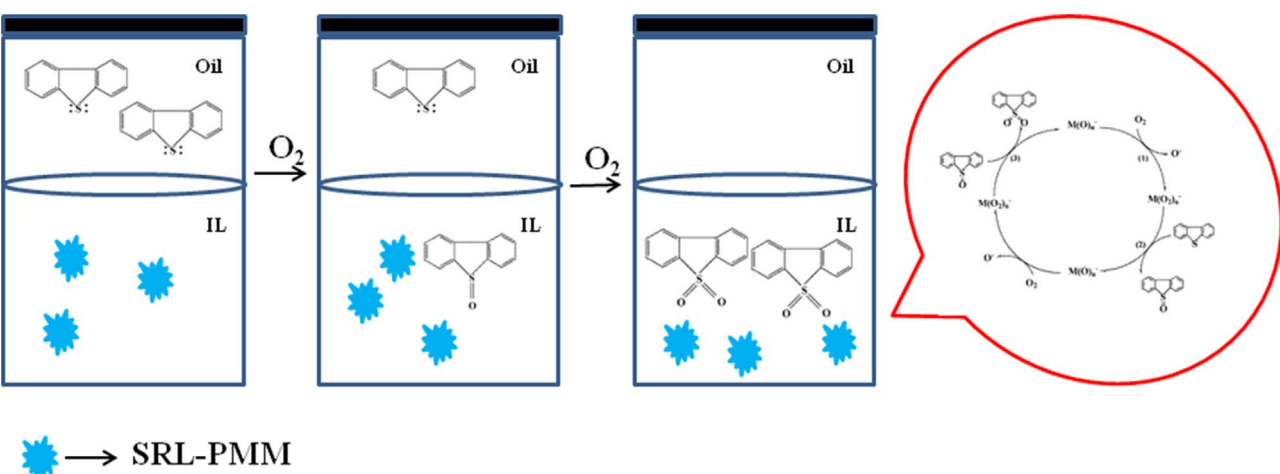


Fig. 12. Oxidative desulfurization system exemplified for the catalyst SRL-PMM.

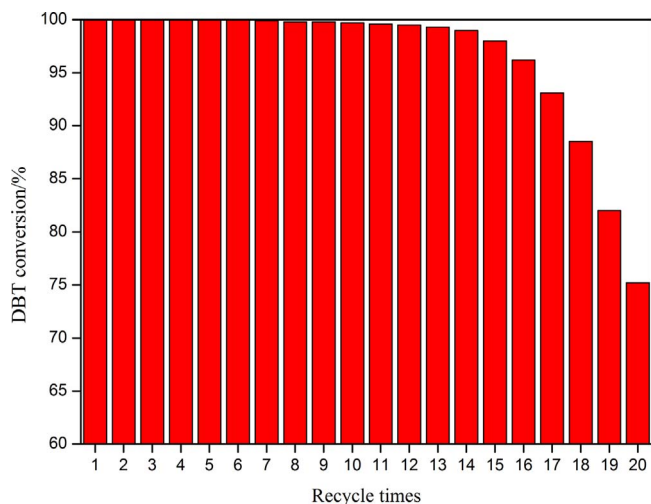


Fig. 13. Stability test results of the catalyst. Conditions: loading amount, 40%; reaction temperature, 60 °C; catalyst dosage, 1.5 g/L; agitation rate, 500 rpm; reaction time, 150 min; O₂ flow rate, 750 ml/min; initial concentration, 2000 ppm.

from 100% to 99%, indicating that SRL-PMM retained its high catalytic activity for ODS even after 14 recycles. After 14 cycles of use, the obvious decrease trend appeared and nearly 25% weight lost. The P content in the catalyst before and after the oxidation reaction was detected by ICP-AES, and weak leaking of SRL-POM was seen in the desulfurization process (mass fraction decreased from 0.39% to 0.37% after reuse 14times). Compared with the other oxidative desulfurization catalysts [33–35], it does show the outstanding recycling characteristic, which can be attributed to the formation of the dual-protection function under porous materials and the stability of the surfactant-type heteropolyacid, SRL-POM.

3.7. Oxidative desulfurization of real oil samples

To investigate whether the catalytic oxidative desulfurization system is effective for real oil samples, the similar studies under commercial oil samples, which was obtained from the Research Institute of Shannxi Yanchang Petroleum Group, was carried out. It was done under optimal experimental conditions: loading amount, 40%; reaction temperature, 60 °C; catalyst dosage, 1.5 g/L; agitation rate, 500 rpm; reaction time, 150 min; O₂ flow rate, 750 ml/min; V([Bmim]BF₄) = 10 ml. The upper phase was withdrawn to analyze and it was found out that the sulfur content decreased from 1500 ppm to nearly 0 ppm (sulfur removal 100%). The color of ionic liquid phase was deepend a

lot and the oil samples became more transparent after the reaction. This suggested that the SRL-PMM had high catalytic oxidative desulfurization activity for the real oil samples.

4. Conclusion

In summary, surfactant-type heteropolyacid (SRL-POM) in the dual-function porous materials, MOF-199 and MCM-41, was successfully synthesized through the one-pot procedure. The XRD, FT-IR, XPS, N₂ adsorption-desorption, SEM, TEM all indicated that the porous materials retained after the introduction of SRL-POM. The SRL-3-PMM displayed significantly a higher catalytic performance under the optimal conditions and shown a better reusability using the as-prepared catalyst and oxygen as the oxidant. This enhanced catalytic performance could be attributed to the good protection measures of porous material supports and the stability of the newly synthesized surfactant-type heteropolyacid. Besides, the kinetic studies reveal that the oxidative desulfurization can present a pseudo first-order kinetic process and the apparent activation energy is 23.7 kJ/mol.

Acknowledgment

We gratefully acknowledge financial support of this work by the National Natural Science Foundation of China (Nos. 21371143, 21671157 and 21501139).

References

- [1] A. Afzalinia, A. Mirzaie, A. Nikseresht, T. Musabeygi, Ultrasound-assisted oxidative desulfurization process of liquid fuel by phosphotungstic acid encapsulated in a interpenetrating amine-functionalized Zn(II)-based MOF as catalyst, *Ulraszon. Sonochem.* 34 (2017) 713–720.
- [2] H. Yang, B. Jiang, Y. Sun, L. Hao, Z. Huang, L. Zhang, Synthesis and oxidative desulfurization of novel lactam-based Brønsted-Lewis acidic ionic liquids, *Chem. Eng. J.* 306 (2016) 131–138.
- [3] D. Piccinino, I. Abdalghani, G. Botta, M. Crucianelli, M. Passacantando, M.L. Di Vacri, R. Saladino, Preparation of wrapped carbon nanotubes poly(4-vinylpyridine)/MTO based heterogeneous catalysts for the oxidative desulfurization (ODS) of model and synthetic diesel fuel, *Appl. Catal. B: Environ.* 200 (2017) 392–401.
- [4] M. Hu, S. Zhao, C. Li, B. Wang, Y. Fu, Y. Wang, Biodesulfurization of vulcanized rubber by enzymes induced from *Gordonia amicalensis*, *Polym. Degrad. Stab.* 128 (2016) 8–14.
- [5] I. Martinez, V.E. Santos, A. Alcon, F. Garcia-Ochoa, Enhancement of the biodesulfurization capacity of *Pseudomonas putida* CECT5279 by co-substrate addition, *Process Biochem.* 50 (2015) 119–124.
- [6] M. Tang, L. Zhou, M. Du, Z. Lyu, X.D. Wen, X. Li, H. Ge, A novel reactive adsorption desulfurization Ni/MnO adsorbent and its hydrodesulfurization ability compared with Ni/ZnO, *Catal. Commun.* 61 (2015) 37–40.
- [7] Y. Xia, Y. Li, Y. Gu, T. Jin, Q. Yang, J. Hu, H. Liu, H. Wang, Adsorption desulfurization by hierarchical porous organic polymer of poly-methylbenzene with metal impregnation, *Fuel* 170 (2016) 100–106.
- [8] F.T. Li, C.G. Kou, Z.M. Sun, Y.J. Hao, R.H. Liu, D.S. Zhao, Deep extractive and

- oxidative desulfurization of dibenzothiophene with C5H9NO-SnCl₂ coordinated ionic liquid, *J. Hazard. Mater.* 205–206 (2012) 164–170.
- [9] H. Ji, J. Sun, P. Wu, B. Dai, Y. Chao, M. Zhang, W. Jiang, W. Zhu, H. Li, Deep oxidative desulfurization with a microporous hexagonal boron nitride confining phosphotungstic acid catalyst, *J. Mol. Catal. A: Chem.* 423 (2016) 207–215.
- [10] A.E.S. Choi, S. Roces, N. Dugos, M.W. Wan, Mixing-assisted oxidative desulfurization of model sulfur compounds using polyoxometalate/H₂O₂ catalytic system, *Sustain. Environ. Res.* 26 (2016) 184–190.
- [11] D. Xie, Q. He, Y. Su, T. Wang, R. Xu, B. Hu, Oxidative desulfurization of dibenzothiophene catalyzed by peroxotungstate on functionalized MCM-41 materials using hydrogen peroxide as oxidant, *Chin. J. Catal.* 36 (2015) 1205–1213.
- [12] K.M. Dooley, D. Liu, A.M. Madrid, F.C. Knopf, Oxidative desulfurization of diesel with oxygen: reaction pathways on supported metal and metal oxide catalysts, *Appl. Catal. A: Gen.* 468 (2013) 143–149.
- [13] H. Zhao, G.A. Baker, Q. Zhang, Design rules of ionic liquids tasked for highly efficient fuel desulfurization by mild oxidative extraction, *Fuel* 189 (2017) 334–339.
- [14] H. Xu, Z. Han, D. Zhang, C. Liu, Theoretical elucidation of the dual role of [HMIm]BF₄ ionic liquid as catalyst and extractant in the oxidative desulfurization of dibenzothiophene, *J. Mol. Catal. A: Chem.* 398 (2015) 297–303.
- [15] M. Zhang, W. Zhu, H. Li, S. Xun, W. Ding, J. Liu, Z. Zhao, Q. Wang, One-pot synthesis, characterization and desulfurization of functional mesoporous W-MCM-41 from POM-based ionic liquids, *Chem. Eng. J.* 243 (2014) 386–393.
- [16] E. Rafiee, S. Rezaei, Deep extractive desulfurization and denitrogenation of various model oils by H₃+nPMo12-nVnO40 supported on silica-encapsulated γ-Fe₂O₃ nanoparticles for industrial effluents applications, *J. Taiwan Inst. Chem. Eng.* 61 (2016) 174–180.
- [17] L. Wang, Y. Chen, L. Du, S. Li, H. Cai, W. Liu, Nickel-heteropolyacids supported on silica gel for ultra-deep desulfurization assisted by ultrasound and ultraviolet, *Fuel* 105 (2013) 353–357.
- [18] C. Jiang, J. Wang, S. Wang, H.y. Guan, X. Wang, M. Huo, Oxidative desulfurization of dibenzothiophene with dioxygen and reverse micellar peroxotitanium under mild conditions, *Appl. Catal. B: Environ.* 106 (2011) 343–349.
- [19] Z.E.A. Abdalla, B. Li, A. Tufail, Direct synthesis of mesoporous (C19H42N)4H₃(PW11O39)/SiO₂ and its catalytic performance in oxidative desulfurization, *Colloids Surf. A: Physicochem. Eng. Asp.* 341 (2009) 86–92.
- [20] Z.E.A. Abdalla, B. Li, Preparation of MCM-41 supported (Bu₄N)4H₃(PW11O39) catalyst and its performance in oxidative desulfurization, *Chem. Eng. J.* 200–202 (2012) 113–121.
- [21] J.-W. Ding, R. Wang, A new green system of HPW@MOFs catalyzed desulfurization using O₂ as oxidant, *Chin. Chem. Lett.* 27 (2016) 655–658.
- [23] D. Julião, A.C. Gomes, M. Pillinger, L. Cunha-Silva, B. de Castro, I.S. Gonçalves, S.S. Balula, Desulfurization of model diesel by extraction/oxidation using a zinc-substituted polyoxometalate as catalyst under homogeneous and heterogeneous (MIL-101(Gr) encapsulated) conditions, *Fuel Process. Technol.* 131 (2015) 78–86.
- [24] S. Ribeiro, A.D.S. Barbosa, A.C. Gomes, M. Pillinger, I.S. Gonçalves, L. Cunha-Silva, S.S. Balula, Catalytic oxidative desulfurization systems based on Keggin phosphotungstate and metal-organic framework MIL-101, *Fuel Process. Technol.* 116 (2013) 350–357.
- [25] S.W. Li, R.M. Gao, R.L. Zhang, J.S. Zhao, Template method for a hybrid catalyst material POM@MOF-199 anchored on MCM-41: highly oxidative desulfurization of DBT under molecular oxygen, *Fuel* 184 (2016) 18–27.
- [26] S.A. Araujo, M. Ionashiro, V.J. Fernandes Jr., A.S. Araujo, Thermogravimetric investigations during the synthesis of silica-based MCM-41, *J. Therm. Anal. Calorim.* 64 (2001) 801–805.
- [27] J. Ge, Y. Zhou, Y. Yang, M. Xue, Catalytic oxidative desulfurization of gasoline using ionic liquid emulsion system, *Ind. Eng. Chem. Res.* 50 (2011) 13686–13692.
- [28] S.O. Ribeiro, D. Julião, L. Cunha-Silva, V.F. Domingues, R. Valença, J.C. Ribeiro, B. de Castro, S.S. Balula, Catalytic oxidative/extractive desulfurization of model and untreated diesel using hybrid based zinc-substituted polyoxometalates, *Fuel* 166 (2016) 268–275.
- [29] L. Yang, J. Li, X. Yuan, J. Shen, Y. Qi, One step non-hydrodesulfurization of fuel oil: catalyzed oxidation adsorption desulfurization over HPWA-SBA-15, *J. Mol. Catal. A: Chem.* 262 (2007) 114–118.
- [30] W. Zhu, P. Wu, Y. Chao, H. Li, F. Zou, S. Xun, F. Zhu, Z. Zhao, A novel reaction-controlled foam-type polyoxometalate catalyst for deep oxidative desulfurization of fuels, *Ind. Eng. Chem. Res.* 52 (2013) 17399–17406.
- [31] J. Qiu, G. Wang, Y. Zhang, D. Zeng, Y. Chen, Direct synthesis of mesoporous H₃PMo12O40/SiO₂ and its catalytic performance in oxidative desulfurization of fuel oil, *Fuel* 147 (2015) 195–202.
- [32] M. Zhang, W. Zhu, S. Xun, H. Li, Q. Gu, Z. Zhao, Q. Wang, Deep oxidative desulfurization of dibenzothiophene with POM-based hybrid materials in ionic liquids, *Chem. Eng. J.* 220 (2013) 328–336.
- [33] J. Xiong, W. Zhu, W. Ding, L. Yang, Y. Chao, H. Li, F. Zhu, H. Li, Phosphotungstic acid immobilized on ionic liquid-modified SBA-15: efficient hydrophobic heterogeneous catalyst for oxidative desulfurization in fuel, *Ind. Eng. Chem. Res.* 53 (2014) 19895–19904.
- [34] M.A. Rezvani, M. Oveis, M.A. Nia Asli, Phosphotungstovanadate immobilized on PVA as an efficient and reusable nano catalyst for oxidative desulphurization of gasoline, *J. Mol. Catal. A: Chem.* 410 (2015) 121–132.